This article was downloaded by:
On: *25 January 2011*
Access details: *Access Details: Free Access*
Publisher *Taylor & Francis*
Informa Ltd Registered in England and Wales Registered Number: 1072954 Registered office: Mortimer House, 37-41 Mortimer Street, London W1T 3JH, UK

Liquid Crystals
Publication details, including instructions for authors and subscription information:
http://www.informaworld.com/smpp/title~content=t713926090

Phase diagrams for a semi-infinite nematic in contact with a micropatterned surface

T. J. Atherton[a]
[a] Department of Physics, Case Western Reserve University, Cleveland, Ohio, USA

Online publication date: 20 October 2010

To cite this Article Atherton, T. J.(2010) 'Phase diagrams for a semi-infinite nematic in contact with a micropatterned surface', Liquid Crystals, 37: 10, 1225 — 1228
To link to this Article: DOI: 10.1080/02678292.2010.493975
URL: http://dx.doi.org/10.1080/02678292.2010.493975

PLEASE SCROLL DOWN FOR ARTICLE

Full terms and conditions of use: http://www.informaworld.com/terms-and-conditions-of-access.pdf

This article may be used for research, teaching and private study purposes. Any substantial or systematic reproduction, re-distribution, re-selling, loan or sub-licensing, systematic supply or distribution in any form to anyone is expressly forbidden.

The publisher does not give any warranty express or implied or make any representation that the contents will be complete or accurate or up to date. The accuracy of any instructions, formulae and drug doses should be independently verified with primary sources. The publisher shall not be liable for any loss, actions, claims, proceedings, demand or costs or damages whatsoever or howsoever caused arising directly or indirectly in connection with or arising out of the use of this material.

Liquid Crystals,
Vol. 37, No. 10, October 2010, 1225–1228

Taylor & Francis
Taylor & Francis Group

Phase diagrams for a semi-infinite nematic in contact with a micropatterned surface

T.J. Atherton*

Department of Physics, Case Western Reserve University, Cleveland, Ohio, USA

(*Received 21 January 2010; final version 13 May 2010*)

Phase diagrams are calculated for the director configuration adopted by a nematic material in contact with a surface micropatterned periodically with homeotropic and planar stripes, and in which an azimuthal easy axis orthogonal to the length of the stripes has been imposed upon the planar stripes. Four stable configurations exist: a uniform homeotropic and a uniform planar state that are preferred when one of the sets of stripes is sufficiently narrow relative to the other, and two distorted states where the director either lies along the length of the stripes or perpendicular to them, depending on the period of the patterning and the polar and azimuthal anchoring coefficients.

Keywords: nematic; micropatterned surfaces; elastic anisotropy; phase diagram

Downloaded At: 13:45 25 January 2011

1. Introduction

Micropatterned surfaces are interesting as a means of arbitrarily controlling the surface orientation of a liquid crystal [1–7], as a route to bistable displays [8, 9] and as a template for smectics [10]. It has recently been shown by the author [1, 11], generalising a theory due to Barbero *et al.* [4], that the known tendency [3] of a striped alternating homeotropic–planar micropatterned surface to align a nematic material along the length of the stripes is due to elastic anisotropy: the twist deformation that occurs if the alignment is along the length of the stripes has, for most nematic materials, a lower energy than the splay and bend deformation imposed by a configuration aligned perpendicular to the stripes. If an azimuthal easy axis is imposed on the planar stripes orthogonal to this elastically preferred direction, then a threshold behaviour is expected. At wavelengths longer than some critical value λ_c, where the anchoring energy dominates, the liquid crystal will follow the imposed easy axis referred to as the 'splay-bend' configuration (Figure 1(a)) while at shorter wavelengths the elastic energy dominates and so the liquid crystal aligns along the length of the stripes referred to as the 'twist' configuration (Figure 1(b)). For typical values [12–14] of the splay (K_1), twist (K_2) and bend (K_3) elastic constants $\sim 10^{-11}$ N, and weak azimuthal anchoring $W_\phi \sim 10^{-6}$ J m^{-2}, the critical wavelength is of micrometre order.

A second sort of orientational transition in the same system has been proposed by Kondrat *et al.* [7]; if either set of stripes are sufficiently narrow relative to the others then the liquid crystal will adopt a uniform bulk configuration. If it is the planar stripes that are very narrow, then the nematic material accordingly adopts a homeotropic configuration (Figure 1(c)) and *vice versa* (Figure 1(d)).

In this work, by constructing expressions for the total energy of all four stable configurations, the complete phase diagram of the semi-infinite nematic liquid crystal in contact with the homeotropic–planar micropatterned surface is evaluated.

2. Model

In order to do so, it is first necessary to evaluate the energy of the distorted states (see Figure 1(a) and (b)). Such an expression was derived in a previous paper [1] to consider the possibility of an azimuthal transition between the distorted states, but omitted a surface term that must be included in order to estimate the absolute value of the free energy. Adopting the coordinate system illustrated in Figure 1, in which the x-axis lies orthogonal to the length of the stripes and the z-axis is perpendicular to the surface, the director field $\hat{\mathbf{n}}$ must be a function of x and z alone and may be parameterised as

$$n = (\cos\theta\cos\phi, \cos\theta\sin\phi, \sin\theta), \tag{1}$$

so the Frank–Oseen elastic energy density

$$f_b = \frac{1}{2}K_{11}(\nabla\cdot\hat{\mathbf{n}})^2 + K_{22}(\hat{\mathbf{n}}\cdot\nabla\times\hat{\mathbf{n}})^2 + K_{33}|\hat{\mathbf{n}}\times\nabla\times\hat{\mathbf{n}}|^2, \tag{2}$$

within the approximation $K_1 = K_3 \neq K_2$ has, as before [1], the form

$$f_{el} = K_1(\kappa\theta_x^2 + \theta_z^2)/2, \tag{3}$$

where $\kappa = [1 - (1-\tau)\sin^2\phi]$, in which $\tau = K_2/K_1$, and the subscripts indicate derivatives taken with respect to

*Email: timothy.atherton@case.edu

ISSN 0267-8292 print/ISSN 1366-5855 online
© 2010 Taylor & Francis
DOI: 10.1080/02678292.2010.493975
http://www.informaworld.com

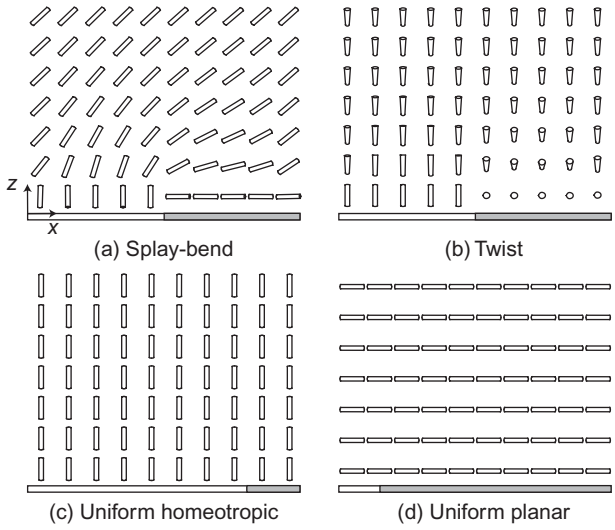

Figure 1. Schematic of the possible configurations adopted by a nematic material in contact with a periodic homeotropic–planar striped surface which has been prepared with an azimuthal easy axis on the planar stripes in the x-direction.

Downloaded At: 13:45 25 January 2011

the appropriate coordinates. The Euler–Lagrange equation for the configuration $\theta(x, z)$ is a scaled version of Laplace's equation,

$$\kappa\theta_{xx} + \theta_{zz} = 0 \tag{4}$$

with the series solution

$$\theta(x,z) = \theta_0 + 2\sum_{n=1}^{\infty} \exp(-2n\pi\sqrt{\kappa}z) \times \left[p_n \sin(2n\pi x) + q_n \cos(2n\pi x)\right], \tag{5}$$

where the coefficients θ_0, p_n and q_n are determined from the boundary condition. By substituting Equation (5) into Equation (3) and integrating, a general expression for the elastic energy per unit length per stripe may be obtained,

$$F_{el} = 2\pi\sqrt{\kappa}\sum_{n=1}^{\infty} n(p_n^2 + q_n^2), \tag{6}$$

where this energy is expressed in units of K_1/λ, which shall be adopted for all subsequent free energies.

For a harmonic anchoring potential

$$W_\theta(\theta - \theta_e)^2/2, \tag{7}$$

where the easy axis θ_e is

$$\theta_e = \begin{cases} \frac{\pi}{2}, & 0 < x \le a, \\ 0, & a < x \le 1, \end{cases} \tag{8}$$

and a is the homeotropic–planar mark-space ratio, the natural boundary condition is

$$\left[\theta_z + 2\frac{\lambda}{L_\theta}(\theta - \theta_e)\right]_{z=0} = 0, \tag{9}$$

where $L_\theta = K_1/(W_\theta\lambda)$ is the characteristic penetration depth of the surface treatment. Substituting Equation (9) into Equation (5) and exploiting the orthogonality of the sin and cos functions, the coefficients

$$\theta_0 = \frac{\pi a}{2},\ p_n = \frac{\sin^2(na\pi)}{2n(1 + 2n\pi\, L_\theta\sqrt{\kappa})},\ q_n = \frac{\sin(2na\pi)}{4n(1 + 2n\pi\, L_\theta\sqrt{\kappa})} \tag{10}$$

are obtained. The bulk elastic energy may be evaluated by substituting Equation (10) into Equation (6):

$$F_{\mathrm{el}}(\kappa, L_\theta) = \pi\sqrt{\kappa}\sum_{n=1}^{\infty}\frac{\sin\,(na\pi)^2}{2n\,(1 + 2n\pi L_\theta\sqrt{\kappa})^2}. \tag{11}$$

The surface anchoring energy, which was not considered in full before [1], is obtained by substituting Equation (5) evaluated at $z = 0$ and Equation (8) into Equation (7) and integrating:

$$F_{\mathrm{surf}}(\kappa, L_\theta) = \frac{1}{2L_\theta}\left[\frac{\pi^2 a}{4}(1 - a) - \sum_{n=1}^{\infty}\frac{(1 + 4n\pi L_\theta\sqrt{\kappa})\sin^2(na\pi)}{2n^2(1 + 2n\pi L_\theta\sqrt{\kappa})^2}\right]. \tag{12}$$

The imposed azimuthal easy axis on the planar stripes, with a characteristic penetration depth $L_\phi = K_1/(W_\phi\lambda)$ where W_ϕ is the azimuthal anchoring coefficient, and within the approximation above that ϕ is constant, has an associated anchoring energy of the Rapini–Papoular form,

$$F_\phi(L_\phi) = \frac{1}{2L_\phi}\int_a^1 \cos^2[\theta(x)]\sin^2(\phi - \phi_e)\,dx, \tag{13}$$

where the azimuthal easy axis $\phi_e = 0$ and where the integral must be evaluated numerically. Note that, since for most surface treatments $L_\phi \gg L_\theta$, the contribution of this potential to the boundary condition for θ (Equation (12)) may be neglected; the θ dependence serves only to reduce the anchoring energy density where the director is more homeotropic.

The total energy per unit length per stripe of the two distorted configurations may now be evaluated using Equations (11)–(13): the energy of the splay-bend configuration, where $\phi = 0$ and so $\kappa = 1$, is

$$F_{\mathrm{splay-bend}} = F_{el}(1, L_\theta) + F_{\mathrm{surf}}(1, L_\theta)$$

and the energy of the twist configuration, where $\phi = \pi/2$ and $\kappa = \tau = K_2/K_1$, is

$$F_{\text{twist}} = F_{\text{el}}(\tau, L_\theta) + F_{\text{surf}}(\tau, L_\theta) + F_\phi(L_\phi).$$

Using the harmonic polar anchoring potential introduced in Equation (7), it is trivial to evaluate the free energy per unit length per stripe of the uniform homeotropic (UH) configuration,

$$F_{\text{UH}} = \frac{1-a}{2L_\theta},$$

and also the uniform planar (UP) configuration,

$$F_{\text{UP}} = \frac{a}{2L_\theta}.$$

3. Results and discussion

Having expressions for the energy of each configuration, it is possible to determine the least energetic state for any given values of the parameters τ, a, L_θ and L_ϕ, and moreover to determine the critical lines that separate the various states. For an experimentally fabricated pattern of $\lambda = 2\mu$m, and using typical values [12–14] for the liquid crystal elastic constant $K_1 \sim 1 \times 10^{-11}$N and polar anchoring energy $W_\theta \sim 1 \times 10^{-4}\text{Jm}^{-2}$, $L_\theta \sim 0.02$; typically, the azimuthal anchoring is an order of magnitude or two weaker and so $L_\phi \gtrsim 0.2$. Two phase diagrams in the τ, a parameter space are plotted in Figure 2 with critical lines for several values of L_θ and L_ϕ, including $L_\phi = \infty$ which corresponds to azimuthally degenerate anchoring on the planar stripes. Notice that the twist state favoured by elastic anisotropy (i.e. for sufficiently small τ) reduces with decreasing τ the width on the a-axis of the uniform phases. Furthermore, Figure 2 suggests that it will be necessary to use a material with rather low polar anchoring energy in order to observe the uniform-distorted transitions.

Experimental observation of these configurations will be limited by the ability of the micropatterning technique to fabricate narrow stripes; photoalignment methods [15] are constrained to the ultraviolet wavelengths while microcontact printing [16] is ultimately constrained by the mask used to make the stamp. A further limitation is that, in the present analysis, variation of the scalar order parameter, S, of the nematic material has been neglected. When the feature size or wavelength becomes comparable to the nematic coherence length then partially melted configurations might represent the ground state.

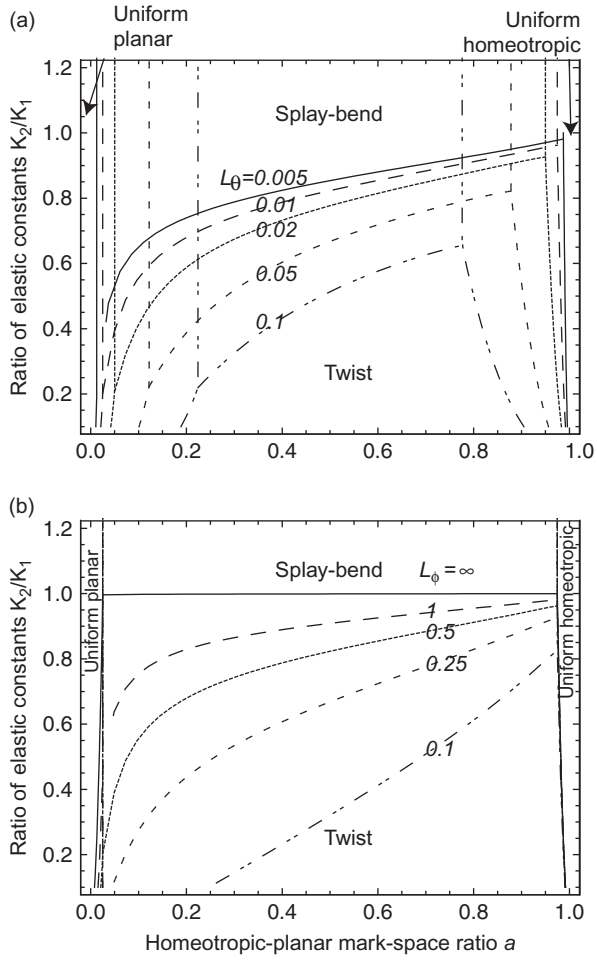

Figure 2. Phase diagrams indicating regions of stability for the four phases: (a) varying the polar anchoring energy fixing $L_\phi = 0.5$; (b) varying the azimuthal anchoring energy fixing $L_\theta = 0.01$

4. Conclusion

A complete phase diagram has been calculated for the semi-infinite nematic material in contact with a micropatterned homeotropic–planar surface of variable period and homeotropic–planar mark-space ratio. Where the 'twist' configuration is favourable, which is the case if the azimuthal anchoring of the antagonistic easy axis on the planar stripes is sufficiently low and if $K_2 < K_1$, the region of stability for the uniform states is reduced. This complex phase behaviour may place constraints on the design of devices that incorporate micropatterned surfaces.

Acknowledgements

The author would like to thank Professor J.R. Sambles for helpful discussions concerning this manuscript.

Downloaded At: 13:45 25 January 2011

References

[1] Atherton, T.J.; Sambles, J.R. *Phys. Rev. E: Stat., Nonlinear, Soft Matter Phys.* **2006**, *74*, 022701.
[2] Atherton, T.J.; Sambles, J.R. *Mol. Cryst. Liq. Cryst.* **2007**, *475*, 3–11.
[3] woon Lee, B.; Clark, N.A. *Science* **2001**, *291* 2576–2580.
[4] Barbero, G.; Beica, T.; Alexe-Ionescu, A.L.; Moldovan, R. *J. Physique II* **1992**, *2*, 2011–2024.
[5] Bechtold, I.H.; Oliveira, E.A. *Liq. Cryst.* **2005**, *32*, 343–347.
[6] Harnau, L.; Kondrat, S.; Poniewierski, A. *Phys. Rev. E: Stat., Nonlinear, Soft Matter Phys.* **2005**, *72*, 011701.
[7] Kondrat, S.; Poniewierski, A.; Harnau, L. *Eur. Phys. J. E* **2003**, *10*, 163–170.
[8] Kim, J.H.; Yoneya, M.; Yokoyama, H. *Nature* **2002**, *420*, 159–162.
[9] Kim, J.H.; Yoneya, J.; Yamamoto, J.; Yokoyama, H. *Appl. Phys. Lett.* **2001**, *78*, 3055–3057.
[10] Bramble, J.; Evans, S.; Henderson, J.; Atherton, T.; Smith, N. *Liq. Cryst.* **2007**, *34*, 1137–1147.
[11] Atherton, T.J.; Sambles, J.R.; Bramble, J.P.; Henderson, J.R.; Evans, S.D.; *Liq. Cryst.* **2009**, *36*, 353–358.
[12] Chandrasekhar, S. *Liquid Crystals*, 2nd ed.; Cambridge University Press, 1992.
[13] *E7 data sheet*, Merck KGaA.
[14] Jewell, S.A.; Sambles, J.R. *J. Appl. Phys.* **2002**, *92*, 19–24.
[15] Schadt, M.; Schmitt, K.; Kozinkov, V.; Chigrinov, V. *Jpn. J. Appl. Phys.* **1992**, *21*, 2155–2164.
[16] Gupta, V.; Abbott, N. *Science* **1997**, *276*, 1533–1536.

Downloaded At: 13:45 25 January 2011